AN UPPER BOUND FOR THE DISTRIBUTION OVERLAP INDEX AND ITS APPLICATIONS

Anonymous authors
Paper under double-blind review

ABSTRACT

The overlap index between two probability distributions has various applications in statistics, machine learning, and other scientific research. However, approximating the overlap index is challenging when the probability distributions are unknown (i.e., distribution-free settings). This paper proposes an easy-to-compute upper bound for the overlap index without requiring any knowledge of the distribution models. We first utilize the bound to find the upper limit for the accuracy of a trained machine learning model when a domain shift exists. We additionally employ this bound to study the distribution membership classification of given samples. Specifically, we build a novel, distribution-free, computation-efficient, memory-efficient one-class classifier by converting the bound into a confidence score function. The proposed classifier does not need to train any parameters and is empirically accurate with only a small number of in-class samples. The classifier shows its efficacy and outperforms many state-of-the-art methods on various datasets in different one-class classification scenarios, including novelty detection, out-of-distribution detection, and backdoor detection. The obtained results show significant promise toward broadening the applications of overlap-based metrics.

1 INTRODUCTION

The distribution overlap index refers to the area intersected by two probability density functions (i.e., Fig. 1(a)) and measures the similarity between the two distributions. A high overlap index value implies a high similarity. Although the overlap index has various applications in many areas, such as biology (Langøy et al., 2012; Utne et al., 2012), economics (Milanovic & Yitzhaki, 2002), and statistics (Inman & Bradley Jr, 1989), the literature on approximating it under distribution-free settings is thin. This work proposes an upper bound for the overlap index with distribution-free settings to broaden the potential applications of overlap-based metrics. The bound is easy to compute and contains three terms: a constant number, the norm of the difference between the two distributions' means, and a variation distance between the two distributions over a subset. Even though finding such an upper bound for the distribution overlap index is already valuable, we further explore two additional applications of our bound as discussed below.

One application of our bound is for domain shift analysis. Specifically, a domain shift is a change in the dataset distribution between a model's training dataset and the testing dataset encountered during implementation (i.e., the overlap index value between the distributions of the two datasets is less than 1). We calculated the model's testing accuracy in terms of the overlap index between the distributions of the training and testing datasets and further found the upper limit of the accuracy using our bound for the overlap index. Knowing the upper bound for a model's testing accuracy helps measure the model's potential and compare it with other models. We validated the calculated upper limit accuracy with experiments in backdoor attacks.

Another application of our bound is for one-class classification. Specifically, one-class classification refers to a model that outputs positive for in-class samples and negative for out-class samples that are absent, poorly sampled, or not well defined (i.e., Fig. 1(b)). We propose a novel one-class classifier by converting our bound into a confidence score function to evaluate if a sample is in-class or out-class. The proposed classifier has many advantages. For example, implementing deep neural network-based classifiers requires training thousands of parameters and large memory, whereas implementing our classifier does not. It only needs sample norms to calculate the confi-

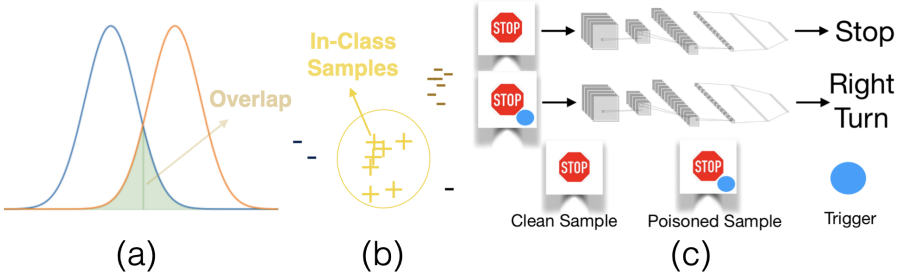

Figure 1: (a): Overlap of two distributions. (b): One-class classification. (c): Backdoor attack.

dence score. Besides, deep neural network-based classifiers need relatively large amounts of data to avoid under-fitting or over-fitting, whereas our method is empirically accurate with only a small number of in-class samples. Therefore, our classifier is computation-efficient, memory-efficient, and data-efficient. Additionally, compared with other traditional one-class classifiers, such as Gaussian distribution-based classifier, Mahalanobis distance-based classifier (Lee et al., 2018) and one-class support vector machine (Schölkopf et al., 2001), our classifier is distribution-free, explainable, and easy to understand.

Overall, the contributions of this paper include:

- Finding a distribution-free upper bound for the overlap index.
- Applying this bound to the domain shift analysis problem with experiments.
- Proposing a novel one-class classifier with the bound being the confidence score function.
- Evaluating the proposed one-class classifier through comparison with various state-of-the-art methods on several datasets, including UCI datasets, CIFAR-100, sub-ImageNet, etc., and in different one-class classification scenarios, such as novelty detection, out-of-distribution detection, and neural network backdoor detection.

1.1 Background and Related Works

Measuring the similarity between distributions: Gini & Livada (1943) and Weitzman (1970) introduced the concept of the distribution overlap index. Other measurements for the similarity between distributions include the total variation distance, Kullback-Leibler divergence (Kullback & Leibler, 1951), Bhattacharyya's distance (Bhattacharyya, 1943), and Hellinger distance (Hellinger, 1909). In psychology, some effect size measures' definitions involve the concept of the distribution overlap index, such as Cohen's U index (Cohen, 2013), McGraw and Wong's CL measure (McGraw & Wong, 1992), and Huberty's I degree of non-overlap index (Huberty & Lowman, 2000). However, they all have strong distribution assumptions (e.g., symmetry or unimodality) regarding the overlap index. Pastore & Calcagnì (2019) approximates the overlap index via kernel density estimators.

One-class classification: Moya & Hush (1996) coined the term one-class classification. One-class classification intersects with novelty detection, anomaly detection, out-of-distribution detection, and outlier detection. Yang et al. (2021) explains the differences among these detection areas. Khan & Madden (2014) discusses many traditional non neural network-based one-class classifiers, such as one-class support vector machine (Schölkopf et al., 2001), decision-tree (Comité et al., 1999), and one-class nearest neighbor (Tax, 2002). Two neural network-based one-class classifiers are (Ruff et al., 2018) and OCGAN (Perera et al., 2019). Morteza & Li (2022) introduces a Gaussian mixture-based energy measurement and compares it with several other score functions, including maximum softmax score (Hendrycks & Gimpel, 2017), maximum Mahalanobis distance (Lee et al., 2018), and energy score (Liu et al., 2020a) for one-class classification.

Neural network backdoor attack and detection: Gu et al. (2019) and Liu et al. (2018b) mentioned the concept of the neural network backdoor attack. The attack contains two steps: during training, the attacker injects triggers into the training dataset; during testing, the attacker leads the network to misclassify by presenting the triggers (i.e., Fig. 1(c)). The data poisoning attack (Biggio et al., 2012) and adversarial attack (Goodfellow et al., 2014) overlap with the backdoor attack. Some proposed

trigger types are Wanet (Nguyen & Tran, 2021), invisible sample-specific (Li et al., 2021), smooth (Zeng et al., 2021), and reflection (Liu et al., 2020b). Some methods protecting neural networks from backdoor attacks include neural cleanse (Wang et al., 2019), fine-pruning (Liu et al., 2018a), and STRIP (Gao et al., 2019). NNoculation (Veldanda et al., 2021) and RAID (Fu et al., 2022) utilize online samples to improve their detection methods. The backdoor detection problem also intersects with one-class classification. Therefore, some one-class classifiers can detect poisoned samples against the neural network backdoor attack.

Organization of the Paper: We first provide preliminaries and derive the proposed upper bound for the overlap index in Sec. 2. We next apply our bound to domain shift analysis in Sec. 3. We then propose, analyze, and evaluate our novel one-class classifier in Sec. 4. We finally conclude the paper in Section 5.

2 An Upper Bound for the Overlap Index

2.1 Preliminaries

For simplicity, we consider the $\mathbb{R}^n$ space and continuous random variables. We also define P and Q as two probability distributions in $\mathbb{R}^n$ with f_P and f_Q being their probability density functions.

Definition 1 (Overlap Index)**.** *The overlap $\eta : \mathbb{R}^n \times \mathbb{R}^n \to [0, 1]$ of the two distributions is defined:*

$$\eta(P, Q) = \int_{\mathbb{R}^n} \min[f_P(x), f_Q(x)]dx. \tag{1}$$

Definition 2 (Total Variation Distance)**.** *The total variation distance $\delta : \mathbb{R}^n \times \mathbb{R}^n \to [0, 1]$ of the two distributions is defined as*

$$\delta(P, Q) = \frac{1}{2} \int_{\mathbb{R}^n} |f_P(x) - f_Q(x)|\, dx. \tag{2}$$

Definition 3 (Variation Distance on Subsets)**.** *Given a subset A from $\mathbb{R}^n$, we define $\delta_A : \mathbb{R}^n \times \mathbb{R}^n \to [0, 1]$ to be the variation distance of the two distributions on A, which is*

$$\delta_A(P, Q) = \frac{1}{2} \int_A |f_P(x) - f_Q(x)|dx. \tag{3}$$

Remark 1. *One can prove that η and δ satisfy the following equation:*

$$\eta(P, Q) = 1 - \delta(P, Q) = 1 - \delta_A(P, Q) - \delta_{\mathbb{R}^n \setminus A}(P, Q). \tag{4}$$

The quantity δ_A defined in (3) will play an important role in deriving our upper bound for η.

2.2 The Upper Bound for the Overlap Index

We now proceed with deriving our proposed upper bound.

Theorem 1. *Without loss of generality, assume D^+ and D^- are two probability distributions on a bounded domain $B \subset \mathbb{R}^n$ with defined norm $||\cdot||$ [1] (i.e., $\sup_{x \in B} ||x|| < +\infty$), then for any subset $A \subset B$ with its complementary set $A^c = B \setminus A$, we have*

$$\eta(D^+, D^-) \leq 1 - \frac{1}{2r_{A^c}} ||\mu_{D^+} - \mu_{D^-}|| - \frac{r_{A^c} - r_A}{r_{A^c}} \delta_A \tag{5}$$

where $r_A = \sup_{x \in A} ||x||$ and $r_{A^c} = \sup_{x \in A^c} ||x||$, μ_{D^+} and μ_{D^-} are the means of D^+ and D^-, and δ_A is the variation distance on set A defined in **Definition** *3. Moreover, let $r_B = \sup_{x \in B} ||x||$, then we have*

$$\eta(D^+, D^-) \leq 1 - \frac{1}{2r_B} ||\mu_{D^+} - \mu_{D^-}|| - \frac{r_B - r_A}{r_B} \delta_A. \tag{6}$$

Since (6) holds for any A, a tighter bound can be written as

$$\eta(D^+, D^-) \leq 1 - \frac{1}{2r_B} ||\mu_{D^+} - \mu_{D^-}|| - \max_A \frac{r_B - r_A}{r_B} \delta_A. \tag{7}$$

[1] In this paper, we use the L_2 norm. However, the choice of the norm is not unique and the analysis can be carried out using other norms as well.

Proof. Let f_{D^+} and f_{D^-} be the probability density functions for D^+ and D^-. From (4), we have

$$\eta(D^+, D^-) = 1 - \delta_A(D^+, D^-) - \delta_{A^c}(D^+, D^-). \tag{8}$$

Using (8), triangular inequality, and boundedness, we obtain

$$||\mu_{D^+} - \mu_{D^-}|| = ||\int_B x\left(f_{D^+}(x) - f_{D^-}(x)\right)dx|| \leq \int_B ||x(f_{D^+}(x) - f_{D^-}(x))||dx \tag{9}$$

$$= \int_A ||x|| \cdot |f_{D^+}(x) - f_{D^-}(x)|dx + \int_{A^c} ||x|| \cdot |f_{D^+}(x) - f_{D^-}(x)|dx \tag{10}$$

$$\leq 2r_A\delta_A + 2r_{A^c}\delta_{A^c} = 2r_A\delta_A + 2r_{A^c}(1 - \delta_A - \eta(D^+, D^-)) \tag{11}$$

which implies (5). Replacing r_{A^c} with r_B in (11) implies (6). □

Remark 2. *The only assumption in this theorem is that the probability distribution domain is bounded. However, almost all real-world applications satisfy the boundedness assumption since the data is bounded. Therefore, r_B can always be found (or at least a reasonable approximation can be found). Additionally, we can constrain A to be a bounded ball so that r_A is also known. Although the proof of this theorem involves probability density functions, the computation does not require knowing the probability density functions but only finite samples because we can use the law of large numbers to estimate $||\mu_{D^+} - \mu_{D^-}||$ and δ_A, which will be shown next.*

2.3 Approximating the Bound with Finite Samples

Let $g : B \to \{0, 1\}$ be a condition function[2] and define $A = \{x \mid g(x) = 1, x \in B\}$. According to the definition of δ_A and triangular inequality, we have

$$\delta_A(D^+, D^-) = \frac{1}{2}\int_A |f_{D^+}(x) - f_{D^-}(x)|dx \geq \frac{1}{2}|\int_A f_{D^+}(x) - f_{D^-}(x)dx| \tag{12}$$

$$= \frac{1}{2}\left|\int_B f_{D^+}(x)g(x)dx - \int_B f_{D^-}(x)g(x)dx\right| = \frac{1}{2}\left|\mathbb{E}_{D^+}[g] - \mathbb{E}_{D^-}[g]\right|. \tag{13}$$

Calculating $\mathbb{E}_{D^+}[g]$ and $\mathbb{E}_{D^-}[g]$ is easy: one just needs to draw samples from D^+ and D^-, and then average their g values. Applying (13) into **Theorem** 1 gives the following corollary:

Corollary 1. *Given D^+, D^-, B, and $||\cdot||$ used in* **Theorem** *1, let $A(g) = \{x \mid g(x) = 1, x \in B\}$ with any condition function $g : B \to \{0, 1\}$. Then, an upper bound for $\eta(D^+, D^-)$ that can be obtained by our approximation is*

$$\eta(D^+, D^-) \leq 1 - \frac{1}{2r_B}||\mu_{D^+} - \mu_{D^-}|| - \max_g \frac{r_B - r_{A(g)}}{2r_B}\left|\mathbb{E}_{D^+}[g] - \mathbb{E}_{D^-}[g]\right|. \tag{14}$$

Given several condition functions $\{g_j\}_{j=1}^k$ and finite sample sets (i.e., $\{x_i^+\}_{i=1}^n \sim D^+$ and $\{x_i^-\}_{i=1}^m \sim D^-$), Alg. 1 shows how to compute the RHS of (14).

Algorithm 1 ComputeBound($\{x_i^+\}_{i=1}^n$, $\{x_i^-\}_{i=1}^m$, $\{g_j\}_{j=1}^k$)

$B \leftarrow \{x_1^+, x_2^+, ..., x_n^+, x_1^-, x_2^-, ..., x_m^-\}$ and $r_B \leftarrow \max_{x \in B} ||x||$
$\Delta_\mu \leftarrow \left|\left|\frac{1}{n}\sum_{i=1}^n x_i^+ - \frac{1}{m}\sum_{i=1}^m x_i^-\right|\right|$
for $j = 1 \to k$ **do**
  $A = \{x \mid g_j(x) = 1, x \in B\}$ and $r_A \leftarrow \max_{x \in A} ||x||$
  $s_j \leftarrow \left(1 - \frac{r_A}{r_B}\right)\left|\frac{1}{n}\sum_{i=1}^n g_j(x_i^+) - \frac{1}{m}\sum_{i=1}^m g_j(x_i^-)\right|$
end for
Return: $1 - \frac{1}{2r_B}\Delta_\mu - \frac{1}{2}\max_j s_j$

Remark 3. *The choice of condition functions is not unique. In this work, we use the indicator function $g(x) = \mathbb{1}\{||x|| \leq r\}$, which outputs 1 if $||x|| \leq r$ and 0 otherwise. By setting different values for r, we generate a family of condition functions. The motivation for choosing such indicator function form is that it is the most simple way to separate a space nonlinearly and it saves computations by directly applying r into* **Corollary 1**. *However, other indicator functions, such as RBF kernel-based indicator functions, are worth exploring and will be considered in our future works.*

[2]The condition function is an indicator function $\mathbb{1}\{condition\}$ that outputs 1 when the input satisfies the given condition and 0 otherwise.

3 APPLICATION OF OUR BOUND TO DOMAIN SHIFT ANALYSIS

We now apply our bound to domain shift analysis.

Theorem 2. *Assume that D and D^* are two different data distributions (i.e., $\eta(D, D^*) < 1$). If a model is trained on D with p accuracy on D and q accuracy on $D^* \setminus D$, then the overall accuracy of the model on D^* is $p\eta(D, D^*) + q(1 - \eta(D, D^*))$, which is upper bounded because $\eta(D, D^*)$ is upper bounded by (14).*

Remark 4. *To prove the theorem, let f_D and f_{D^*} be their probability density functions, then*

$$Accuracy = \int_{x \sim D^*} \left(p \frac{\min\{f_D(x), f_{D^*}(x)\}}{f_{D^*}(x)} + q \left(1 - \frac{\min\{f_D(x), f_{D^*}(x)\}}{f_{D^*}(x)} \right) \right) f_{D^*}(x) dx \quad (15)$$

$$= p\eta(D, D^*) + q(1 - \eta(D, D^*)) = (p - q)\eta(D, D^*) + q. \quad (16)$$

Without loss of generality, assume $p > q$. Then (16) shows that a large domain shift (i.e., a small $\eta(D, D^*)$) leads to low overall accuracy of the model on the testing data distribution D^*. If $p = 1$ and $q = 0$, then the overall accuracy is equal to $\eta(D, D^*)$.

Theorem 2 in Backdoor Attack Scenarios: A backdoor attack scenario (Fig. 1(b)) considers that the model has a zero accuracy on poisoned data distribution as the attack success rate is almost 100%. Define the clean data distribution as D, poisoned data distribution as D^p, and a testing data distribution D^* composed by D and D^p, i.e., $D^* = \sigma D + (1 - \sigma) D^p$, where $\sigma \in [0, 1]$ is the purity ratio (i.e., the ratio of clean samples to the entire testing samples). With all the settings above, we know that $q = 0$ on D^p and equation 16 becomes

$$Accuracy = p\eta(D, D^*) \leq p(1 - \frac{1}{2r_B} ||\mu_D - \mu_{D^*}|| - \max_g \frac{r_B - r_{A(g)}}{2r_B} |\mathbb{E}_D[g] - \mathbb{E}_{D^*}[g]|) \quad (17)$$

$$= p(1 - \frac{1 - \sigma}{2r_B} ||\mu_D - \mu_{D^p}|| - (1 - \sigma) \max_g \frac{r_B - r_{A(g)}}{2r_B} |\mathbb{E}_D[g] - \mathbb{E}_{D^p}[g]|). \quad (18)$$

17 shows that the actual model accuracy on the contaminated testing data should be bounded by the multiplication of its accuracy p on clean data and our upper bound for $\eta(D, D^*)$ with samples. 18 shows that the upper limit of the model accuracy on the contaminating data should linearly increase with the purity ratio σ (i.e., the percentage of clean samples over the entire testing samples).

Validation: Four different datasets (MNIST (LeCun et al., 2010), GTSRB (Stallkamp et al., 2011), GTSRB (Stallkamp et al., 2011), YouTube Face (Wolf et al., 2011), and sub-ImageNet (Deng et al., 2009)) were considered. We composed our testing datasets D^* with $\sigma = 0, 0.1, ..., 0.9, 1$ and calculated the upper bound for $\eta(D, D^*)$ using L_1, L_2, and L_∞ norms in the raw data space, model output space, and intermediate layer space. The actual model accuracy and corresponding upper bounds are plotted in Fig. 2. The actual model accuracy is below all the calculated upper limits, validating **Theorem** 2. Additionally, the upper limits grow linearly with σ, supporting 18. In other scenarios except for backdoor attack, the model accuracy, p, and q may be known, then the lower bound for η can be estimated by **Theorem** 2. **Theorem** 2 can also help in finding q by knowing p, η, and model accuracy. Therefore, **Theorem** 2 has practical relevance and usefulness.

4 APPLICATION OF OUR BOUND TO ONE-CLASS CLASSIFICATION

4.1 PROBLEM FORMULATION FOR ONE-CLASS CLASSIFICATION

Given $\mathbb{R}^d$ space and n samples $\{x_i\}_{i=1}^n$ that lie in an unknown probability distribution, we would like to build a test $\Psi : \mathbb{R}^d \to \{\pm 1\}$ so that for any new input x, $\Psi(x)$ outputs 1 when x is from the same unknown probability distribution, and outputs -1, otherwise. Some applications of Ψ are novelty detection, out-of-distribution detection, and backdoor detection (e.g., Fig. 1(b, c)).

4.2 A NOVEL CONFIDENCE SCORE FUNCTION

Given some in-class samples $\{x_i\}_{i=1}^n$, one can pick several condition functions $\{g_j\}_{j=1}^k$, where $g_j(x) = \mathbb{1}\{||x|| \leq r_j\}$ for different r_j, so that $f(x) = ComputeBound(\{x\}, \{x_i\}_{i=1}^n, \{g_j\}_{j=1}^k)$ defined in Alg. 1 is a score function that measures the likelihood of any input, x, being an in-class sample. Alg. 2 shows the overall one-class classification algorithm.

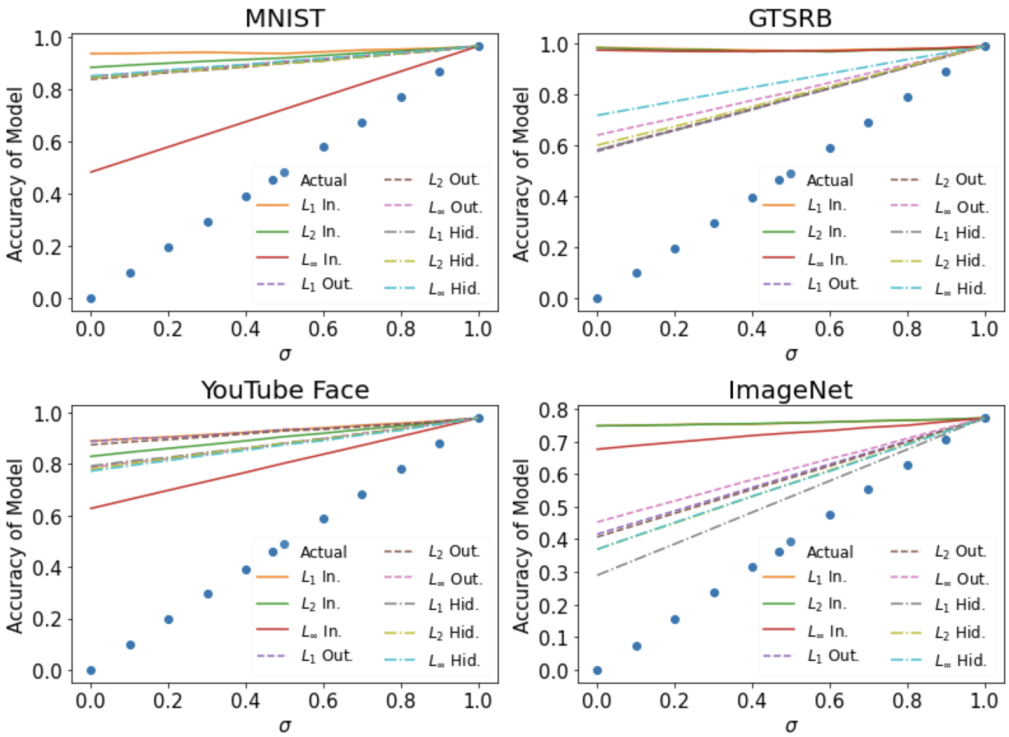

Figure 2: The actual model accuracy (dot) vs. equation 16 (solid) calculated with L_1, L_2, and L_∞ norms in input, output, and hidden spaces. x: the ratio of clean samples to the entire testing samples.

Algorithm 2 The Novel One-Class Classifier for the Input x

Given in-class samples $\{x_i\}_{i=1}^n$, select several condition functions $\{g_j\}_{j=1}^k$, set a threshold T_0
if $ComputeBound(\{x\}, \{x_i\}_{i=1}^n, \{g_j\}_{j=1}^k) \geq T_0$ **then**
  x is an in-class sample
else
  x is an out-class sample
end if

Remark 5. *The score function f measures the maximum similarity between the new input x and the available in-class samples $\{x_i\}_{i=1}^n$. Different T_0 lead to different detection accuracy. However, we will show that the proposed one-class classifier has an overall high accuracy under different T_0.*

4.3 Computation and Space Complexities

Our algorithm can pre-compute and store $\frac{1}{n}\sum_{i=1}^n x_i$ and $\frac{1}{n}\sum_{i=1}^n g_j(x_i)$ with $j = 1, 2, ..., k$. Therefore, the total space complexity is $\mathcal{O}(k+1)$. Assume that the total number of new online inputs is l; then, for every new input x, our algorithm needs to calculate $||x||$ once and s_j for k times. Therefore, the total computation complexity is $\mathcal{O}(l(k+1))$. Empirically, we restricted k to be a small number (e.g., 10) so that even devices without strong computation power can run our algorithm efficiently. Therefore, our classifier is computation-efficient and memory-efficient. The corresponding experimental results will be provided in the following subsection.

4.4 Evaluation

Overall Setup: All the baseline algorithms with optimal hyperparameters, related datasets, and models were acquired from the corresponding authors' websites. The only exception is backdoor

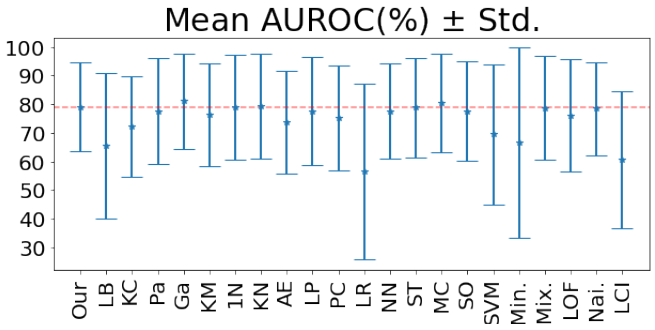

Figure 3: The method is listed in the same order as in Table 3.

detection, in which we created our own models. However, we have carefully fine-tuned the baseline methods' hyperparameters to ensure their best performance over other hyperparameter choices.

4.4.1 One-Class Classification for Novelty Detection

We evaluated our classifier on 100 small UCI datasets (UCI; Dua & Graff, 2017) and recorded the area under the receiver operating characteristic curve (AUROC). Fig. 3 shows the mean and standard deviation of AUROC for ours and other classifiers. Detailed numerical results can be found in Table 3 in Appendix A. The implementation code is provided in the supplementary material.

Our classifier is the most consistent with the smallest standard deviation. Except for *Gaussian*, *K-Nearest Neighbor*, and *Minimum Covariance Determinant*, our classifier outperforms the other methods by showing the highest AUROC mean and the lowest AUROC standard deviation. Among *Gaussian*, *K-Nearest Neighbor*, and *Minimum Covariance Determinant*, *Gaussian* is the best classifier by having the highest mean and lowest standard deviation of AUROC. However, our method is comparable to *Gaussian* by showing a close mean and a smaller standard deviation.

Besides the results, our classifier is distribution-free, computation-efficient, and memory-efficient, whereas some other classifiers do not. Additionally, our method is also easy to explain and understand: the score measures the maximum similarity between the new input and the available in-class samples. Therefore, we conclude that our classifier is valid for novelty detection.

4.4.2 One-Class Classification for Out-of-Distribution Detection

We used CIFAR-10 and CIFAR-100 testing datasets (Krizhevsky et al., 2009) as the in-distribution datasets. The compared methods contain MSP (Hendrycks & Gimpel, 2017), Mahalanobis (Lee et al., 2018), Energy score (Liu et al., 2020a), and GEM (Morteza & Li, 2022). We used WideResNet (Zagoruyko & Komodakis, 2016) to extract features from the raw data. The WideResNet models (well-trained on CIFAR-10 and CIFAR-100 training datasets) and corresponding feature extractors were acquired from (Morteza & Li, 2022). All the methods were evaluated in the same feature spaces with their optimal hyperparameters for fair comparisons. To fit the score function's parameters for all the methods, we formed a small dataset by randomly selecting 10 samples from each class. The out-of-distribution datasets include Textures (Cimpoi et al., 2014), SVHN (Netzer et al., 2011), LSUN-Crop (Yu et al., 2015), LSUN-Resize (Yu et al., 2015), and iSUN (Xu et al., 2015). We used three metrics: the detection accuracy for out-of-distribution samples when the detection accuracy for in-distribution samples is 95% (TPR95), AUROC, and area under precision and recall (AUPR).

Table 1 shows the average results for CIFAR-10 and CIFAR-100. The details for each individual out-of-distribution dataset can be found in Table 4 and Table 5 in Appendix B. Our method outperforms the other methods by using the least memory and showing the highest AUROC on average. Our approach is also one of the fastest methods: the execution time of our approach for each sample is less than one millisecond (ms). For the CIFAR-10 case, our method also shows the highest average TPR95, and the average AUPR of our method is over 92%. For the CIFAR-100 case, the average TPR95 of our method is 0.3% close to the highest average TPR95, and the average AUPR of our method is over 85%. For each individual out-of-distribution dataset, our method always outperforms no less than half of the methods in TPR95 and AUROC, and the total average AUPR

Table 1: Average performance on various out-of-distribution datasets.

In-Distributions	Method	TPR95	AUROC	AUPR	Time/Sample	Memory
CIFAR-10	Ours	**72.33%**	**92.76%**	92.32%	0.60ms	**1048.22MiB**
	MSP	50.63%	91.46%	**98.07%**	**0.02ms**	1825.21MiB
	Mahala.	46.83%	90.46%	97.92%	30.61ms	1983.17MiB
	Energy	68.31%	92.32%	97.96%	0.22ms	1830.01MiB
	GEM	50.81%	90.45%	97.91%	25.62ms	1983.51MiB
CIFAR-100	Ours	48.08	**87.63**	85.72	0.60ms	**1134.32MiB**
	MSP	19.87	75.97	94.09	**0.02ms**	1825.98MiB
	Mahala.	48.35	84.90	96.37	56.24ms	1983.81MiB
	Energy	27.91	80.44	95.15	0.21ms	1838.23MiB
	GEM	**48.36**	84.94	**96.38**	56.27ms	1984.77MiB

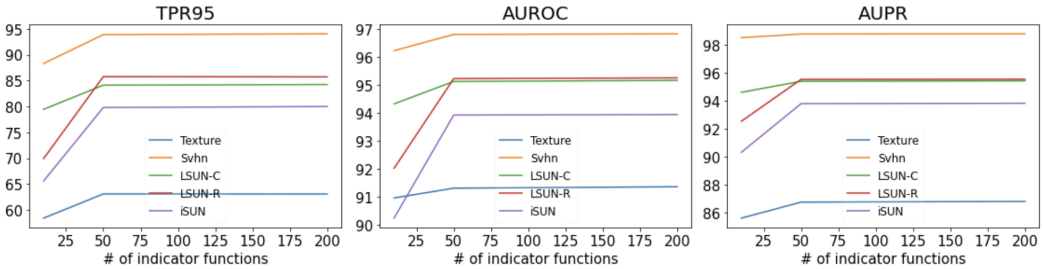

Figure 4: Improvements with more indicator functions.

of our method over all cases is 89.02%. We noticed that the out-of-distribution datasets are much smaller in size than the in-distribution datasets. Therefore, although the current AUPR is sufficient to ensure that our approach is valid, we see a potential improvement in our method to increase the AUPR for heavily imbalanced problems in our prospective work. On balanced datasets shown in Table 2, our approach shows higher AUPR than the baseline methods. Therefore, our approach performs better on balanced datasets than on unbalanced datasets. We also empirically observed that the compared baseline methods reported errors when data dimensions are dependent because the compared baseline methods need to calculate the inverse of the estimated covariance matrices that will not be full rank if data dimensions are dependent. We have reported this observation in Table 6 in the appendix. In contrast, our approach works since it does not require finding the inverse of any matrices. Further, Table 1 and Table 2 together show that the baseline methods perform well only for out-of-distribution detection, whereas our approach performs well for both out-of-distribution detection and backdoor detection (details are explained in next subsection). In summary, our classifier is a valid out-of-distribution detector.

Discussion on Improvements: We evaluated our approach by using more indicator functions (i.e., more r_i) and plotted the results in Fig. 4. From the figure, the performance of our approach increases with more indicator functions being used and eventually converges. Additionally, the limit for each dataset in Fig. 4 is determined by the form of utilized indicator functions, which is $g(x) = \mathbb{1}\{||x|| \leq r\}$ in this work. To increase the limit, more advanced indicator functions are required, which is mentioned in **Remark** 3 that exploring other indicator functions will be our future works.

4.4.3 One-Class Classification for Backdoor Detection

The utilized datasets are MNIST (LeCun et al., 2010), CIFAR-10 (Krizhevsky et al., 2009), GTSRB (Stallkamp et al., 2011), YouTube Face (Wolf et al., 2011), and sub-ImageNet (Deng et al., 2009). The adopted backdoor attacks include naive triggers, all-label attacks (Gu et al., 2019), moving triggers (Fu et al., 2020), Wanet (Nguyen & Tran, 2021), combination attacks, large-sized triggers, filter triggers, and invisible sample-specific triggers (Li et al., 2021), as listed in Fig. 5. The neural network architecture includes Network in Network (Lin et al., 2014), Resnet (He et al., 2016), and

Table 2: Average performance for backdoor detection over various backdoor triggers and datasets.

Metrics (%)	Ours	STRIP	Mahalanobis	GEM	MSP
TPR95	89.40	39.60	56.97	**91.57**	39.24
AUROC	**96.68**	70.30	75.94	58.08	54.92
AUPR	**95.42**	68.76	76.37	75.88	60.52

other networks from (Wang et al., 2019; Gu et al., 2019). For each backdoor attack, we assume that a small clean validation dataset is available (i.e., 10 samples from each class) at the beginning. Therefore, the poisoned samples (i.e., samples attached with triggers) can be considered out-class samples, whereas the clean samples can be considered in-class samples. We used the backdoored network to extract data features. Then, we evaluated our one-class classifier and compared it with the previous baseline methods and STRIP (Gao et al., 2019) in the feature space. The metrics used are the same: TPR95 (i.e., the detection accuracy for poisoned samples when the detection accuracy for clean samples is 95%), AUROC, and AUPR. Table 2 shows the average performance. Details on each individual trigger can be found in Table 6 in Appendix C

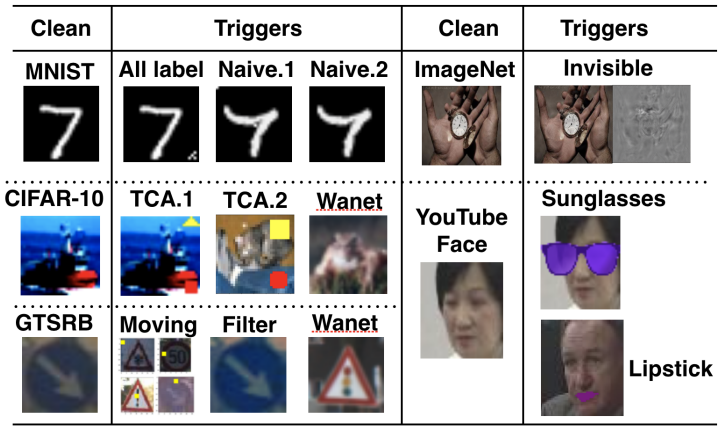

Figure 5: Pictures under "Triggers" are poisoned samples regarding different backdoored attacks. Pictures under "Clean" are clean samples for each dataset.

From the table, our classifier outperforms other baseline methods on average by showing higher AUROC, and AUPR. As for TPR95, our approach is very close to GEM. Compared with STRIP on the overall average performance, our classifier is 49.8% higher in TPR95, 26.38% higher in AUROC, and 26.66% higher in AUPR. For each individual trigger, the TPR95 of our method is over 96% for most cases, the AUROC of our method is over 97% for most cases, and the AUPR of our method is over 95% for most cases. It is also seen that our classifier is robust against the latest or advanced backdoor attacks, such as Wanet, invisible trigger, all label attack, and filter attack, whereas the baseline methods show low performance on those attacks. Therefore, we conclude that our classifier is valid for backdoor detection.

5 Conclusion

This paper proposes an easy-to-compute distribution-free upper bound for the distribution overlap index. Two applications of the bound are explored. The first application is for domain shift analysis with a proposed theorem and discussion. The second application is for one-class classification. Specifically, this paper introduces a novel distribution-free one-class classifier with the bound being its confidence score function. The classifier is sample-efficient, computation-efficient, and memory-efficient. The proposed classifier is evaluated on novelty detection, out-of-distribution detection, and backdoor detection on various datasets and compared with many state-of-the-art methods. The obtained results show significant promise toward broadening the application of overlap-based metrics.

REFERENCES

One-class classifier results. http://homepage.tudelft.nl/n9d04/occ/index.html. Accessed: 2022-08-30.

Anil Bhattacharyya. On a measure of divergence between two statistical populations defined by their probability distributions. *Bulletin of the Calcutta Mathematical Society*, 35:99–109, 1943.

Battista Biggio, Blaine Nelson, and Pavel Laskov. Poisoning attacks against support vector machines. In *Proceedings of the International Conference on International Conference on Machine Learning*, pp. 1467–1474, Edinburgh, Scotland, June 2012.

Mircea Cimpoi, Subhransu Maji, Iasonas Kokkinos, Sammy Mohamed, and Andrea Vedaldi. Describing textures in the wild. In *Proceedings of the IEEE Conference on Computer Vision and Pattern Recognition*, pp. 3606–3613, Columbus, OH, June 2014.

Jacob Cohen. *Statistical power analysis for the behavioral sciences*. Routledge, 2013.

Francesco De Comité, François Denis, Rémi Gilleron, and Fabien Letouzey. Positive and unlabeled examples help learning. In *Proceedings of International Conference on Algorithmic Learning Theory*, pp. 219–230, Tokyo, Japan, Dec. 1999.

J. Deng, W. Dong, R. Socher, L. Li, Kai Li, and Li Fei-Fei. Imagenet: A large-scale hierarchical image database. In *Proceedings of the IEEE Conference on Computer Vision and Pattern Recognition*, pp. 248–255, Miami, FL, 2009.

Dheeru Dua and Casey Graff. UCI machine learning repository, 2017. URL http://archive.ics.uci.edu/ml.

Hao Fu, Akshaj Kumar Veldanda, Prashanth Krishnamurthy, Siddharth Garg, and Farshad Khorrami. Detecting backdoors in neural networks using novel feature-based anomaly detection. *arXiv preprint arXiv:2011.02526*, 2020.

Hao Fu, Akshaj Kumar Veldanda, Prashanth Krishnamurthy, Siddharth Garg, and Farshad Khorrami. A feature-based on-line detector to remove adversarial-backdoors by iterative demarcation. *IEEE Access*, 10:5545 – 5558, 2022.

Yansong Gao, Change Xu, Derui Wang, Shiping Chen, Damith C Ranasinghe, and Surya Nepal. Strip: A defence against trojan attacks on deep neural networks. In *Proceedings of the Annual Computer Security Applications Conference*, pp. 113–125, Austin, TX, Dec. 2019.

C Gini and G Livada. Nuovi contributi alla teoria della transvariazione. *Roma: Atti della VI Riunione della Società Italiana di Statistica*, 1943.

Ian Goodfellow, Jean Pouget-Abadie, Mehdi Mirza, Bing Xu, David Warde-Farley, Sherjil Ozair, Aaron Courville, and Yoshua Bengio. Generative adversarial nets. In *Proceedings of Advances in Neural Information Processing Systems*, volume 27, Montreal, Canada, Dec. 2014.

Tianyu Gu, Kang Liu, Brendan Dolan-Gavitt, and Siddharth Garg. Badnets: Evaluating backdooring attacks on deep neural networks. *IEEE Access*, 7:47230–47244, 2019.

Kaiming He, Xiangyu Zhang, Shaoqing Ren, and Jian Sun. Deep residual learning for image recognition. In *Proceedings of the IEEE Conference on Computer Vision and Pattern Recognition*, pp. 770–778, Miami, FL, June 2016.

Ernst Hellinger. Neue begründung der theorie quadratischer formen von unendlichvielen veränderlichen. *Journal für die reine und angewandte Mathematik*, 1909(136):210–271, 1909.

Dan Hendrycks and Kevin Gimpel. A baseline for detecting misclassified and out-of-distribution examples in neural networks. In *Proceedings of International Conference on Learning Representations*, Toulon, France, Apr. 2017.

Carl J Huberty and Laureen L Lowman. Group overlap as a basis for effect size. *Educational and Psychological Measurement*, 60(4):543–563, 2000.

Henry F Inman and Edwin L Bradley Jr. The overlapping coefficient as a measure of agreement between probability distributions and point estimation of the overlap of two normal densities. *Communications in Statistics-theory and Methods*, 18(10):3851–3874, 1989.

Shehroz S Khan and Michael G Madden. One-class classification: taxonomy of study and review of techniques. *The Knowledge Engineering Review*, 29(3):345–374, 2014.

Alex Krizhevsky, Geoffrey Hinton, et al. Learning multiple layers of features from tiny images, 2009.

Solomon Kullback and Richard A Leibler. On information and sufficiency. *The Annals of Mathematical Statistics*, 22(1):79–86, 1951.

Herdis Langøy, Leif Nøttestad, Georg Skaret, Cecilie Broms, and Anders Fernö. Overlap in distribution and diets of atlantic mackerel (scomber scombrus), norwegian spring-spawning herring (clupea harengus) and blue whiting (micromesistius poutassou) in the norwegian sea during late summer. *Marine Biology Research*, 8(5-6):442–460, 2012.

Yann LeCun, Corinna Cortes, and CJ Burges. Mnist handwritten digit database. *ATT Labs [Online]. Available: http://yann.lecun.com/exdb/mnist*, 2, 2010.

Kimin Lee, Kibok Lee, Honglak Lee, and Jinwoo Shin. A simple unified framework for detecting out-of-distribution samples and adversarial attacks. In *Proceedings of Advances in Neural Information Processing Systems*, volume 31, Montreal, Canada, Dec. 2018.

Yuezun Li, Yiming Li, Baoyuan Wu, Longkang Li, Ran He, and Siwei Lyu. Invisible backdoor attack with sample-specific triggers. In *Proceedings of the IEEE/CVF International Conference on Computer Vision*, pp. 16463–16472, Virtual, June 2021.

Min Lin, Qiang Chen, and Shuicheng Yan. Network in network. In *Proceedings of the International Conference on Learning Representations*, pp. 1–10, Banff, Canada, Apr. 2014.

Kang Liu, Brendan Dolan-Gavitt, and Siddharth Garg. Fine-pruning: Defending against backdooring attacks on deep neural networks. In *Proceedings of International Symposium on Research in Attacks, Intrusions, and Defenses*, pp. 273–294, Crete, Greece, Sep. 2018a.

Weitang Liu, Xiaoyun Wang, John Owens, and Yixuan Li. Energy-based out-of-distribution detection. In *Proceedings of Advances in Neural Information Processing Systems*, volume 33, pp. 21464–21475, Virtual, Dec. 2020a.

Yingqi Liu, Shiqing Ma, Yousra Aafer, Wen-Chuan Lee, Juan Zhai, Weihang Wang, and Xiangyu Zhang. Trojaning attack on neural networks. In *Proceedings of the Network and Distributed Systems Security Symposium*, San Diego, CA, Feb. 2018b.

Yunfei Liu, Xingjun Ma, James Bailey, and Feng Lu. Reflection backdoor: A natural backdoor attack on deep neural networks. In *Proceedings of the European Conference on Computer Vision*, pp. 182–199, Virtual, Aug. 2020b.

Kenneth O McGraw and Seok P Wong. A common language effect size statistic. *Psychological Bulletin*, 111(2):361, 1992.

Branko Milanovic and Shlomo Yitzhaki. Decomposing world income distribution: Does the world have a middle class? *Review of Income and Wealth*, 48(2):155–178, 2002.

Peyman Morteza and Yixuan Li. Provable guarantees for understanding out-of-distribution detection. In *Proceedings of the AAAI Conference on Artificial Intelligence*, volume 8, Virtual, Feb. 2022.

Mary M Moya and Don R Hush. Network constraints and multi-objective optimization for one-class classification. *Neural Networks*, 9(3):463–474, 1996.

Yuval Netzer, Tao Wang, Adam Coates, Alessandro Bissacco, Bo Wu, and Andrew Y Ng. Reading digits in natural images with unsupervised feature learning. In *Proceedings of NIPS Workshop on Deep Learning and Unsupervised Feature Learning*, Granada, Spain, Dec. 2011.

Tuan Anh Nguyen and Anh Tuan Tran. Wanet - imperceptible warping-based backdoor attack. In *Proceedings of the International Conference on Learning Representations*, Virtual, May 2021.

Massimiliano Pastore and Antonio Calcagnì. Measuring distribution similarities between samples: A distribution-free overlapping index. *Frontiers in Psychology*, 10:1089, 2019.

Pramuditha Perera, Ramesh Nallapati, and Bing Xiang. Ocgan: One-class novelty detection using gans with constrained latent representations. In *Proceedings of the IEEE/CVF Conference on Computer Vision and Pattern Recognition*, pp. 2898–2906, Long Beach, CA, June 2019.

Lukas Ruff, Robert Vandermeulen, Nico Goernitz, Lucas Deecke, Shoaib Ahmed Siddiqui, Alexander Binder, Emmanuel Müller, and Marius Kloft. Deep one-class classification. In *Proceedings of International Conference on Machine Learning*, pp. 4393–4402, Stockholm , Sweden, July 2018.

Bernhard Schölkopf, John C Platt, John Shawe-Taylor, Alex J Smola, and Robert C Williamson. Estimating the support of a high-dimensional distribution. *Neural Computation*, 13(7):1443–1471, 2001.

Johannes Stallkamp, Marc Schlipsing, Jan Salmen, and Christian Igel. The german traffic sign recognition benchmark: A multi-class classification competition. In *Proceedings of the International Joint Conference on Neural Networks*, pp. 1453–1460, San Jose, CA, July 2011.

David Martinus Johannes Tax. *One-class classification: Concept learning in the absence of counter-examples*. PhD thesis, Technische Universiteit Delft, 2002.

Kjell Rong Utne, Geir Huse, Geir Ottersen, Jens Christian Holst, Vladimir Zabavnikov, Jan Arge Jacobsen, Gumundur J Óskarsson, and Leif Nøttestad. Horizontal distribution and overlap of planktivorous fish stocks in the norwegian sea during summers 1995–2006. *Marine Biology Research*, 8(5-6):420–441, 2012.

Akshaj Kumar Veldanda, Kang Liu, Benjamin Tan, Prashanth Krishnamurthy, Farshad Khorrami, Ramesh Karri, Brendan Dolan-Gavitt, and Siddharth Garg. Nnoculation: Catching badnets in the wild. In *Proceedings of the ACM Workshop on Artificial Intelligence and Security*, pp. 49–60, Virtual, Nov. 2021.

Bolun Wang, Yuanshun Yao, Shawn Shan, Huiying Li, Bimal Viswanath, Haitao Zheng, and Ben Y Zhao. Neural cleanse: Identifying and mitigating backdoor attacks in neural networks. In *Proceedings of IEEE Symposium on Security and Privacy*, pp. 707–723, San Francisco, CA, May 2019.

Murray S Weitzman. *Measures of overlap of income distributions of white and Negro families in the United States*, volume 3. US Bureau of the Census, 1970.

Lior Wolf, Tal Hassner, and Itay Maoz. Face recognition in unconstrained videos with matched background similarity. In *Proceedings of the IEEE Conference on Computer Vision and Pattern Recognition*, pp. 529–534, Colorado Springs, CO, June 2011.

Pingmei Xu, Krista A Ehinger, Yinda Zhang, Adam Finkelstein, Sanjeev R Kulkarni, and Jianxiong Xiao. Turkergaze: Crowdsourcing saliency with webcam based eye tracking. *arXiv preprint arXiv:1504.06755*, 2015.

Jingkang Yang, Kaiyang Zhou, Yixuan Li, and Ziwei Liu. Generalized out-of-distribution detection: A survey. *arXiv preprint arXiv:2110.11334*, 2021.

Fisher Yu, Ari Seff, Yinda Zhang, Shuran Song, Thomas Funkhouser, and Jianxiong Xiao. Lsun: Construction of a large-scale image dataset using deep learning with humans in the loop. *arXiv preprint arXiv:1506.03365*, 2015.

Sergey Zagoruyko and Nikos Komodakis. Wide residual networks. *arXiv preprint arXiv:1605.07146*, 2016.

Yi Zeng, Won Park, Z Morley Mao, and Ruoxi Jia. Rethinking the backdoor attacks' triggers: A frequency perspective. In *Proceedings of the IEEE/CVF International Conference on Computer Vision*, pp. 16473–16481, 2021.

A DETAILS FOR NOVELTY DETECTION

The method in Table 3 is in the same order as shown in Fig. 3.

Table 3: Means and standard deviations of AUROC (%) for different methods on 100 UCI datasets.

Ours	L1-Ball	K-Center	Parzen	Gaussian	K-Mean
79 ± 15.6	65.4 ± 25.4	72.2 ± 17.6	77.6 ± 18.6	81.1 ± 16.6	76.3 ± 17.9
1-Nearest Neighbor	K-Nearest Neighbor	Auto-Encoder Network	Linear Programming	Principal Component	Lof Range
78.8 ± 18.3	79.2 ± 18.3	73.7 ± 17.9	77.5 ± 18.9	75.1 ± 18.3	56.5 ± 30.8
Nearest Neighbor Distance	Minimum Spanning Tree	Minimum Covariance Determinant	Self Organizing Map	Support Vector Machine	Minimax Probability Machine
77.5 ± 16.6	78.8 ± 17.4	80.4 ± 17.1	77.6 ± 17.4	69.4 ± 24.6	66.4 ± 33.3
Mixture Gaussians	Local Outlier Factor	Naive Parzen	Local Correlation Integral		
78.7 ± 18.1	76.1 ± 19.7	78.4 ± 16.2	60.7 ± 23.9		

B DETAILS FOR OUT-OF-DISTRIBUTION DETECTION

Table 4 is for CIFAR-10 case and Table 5 is for CIFAR-100 case.

C DETAILS FOR BACKDOOR DETECTION

Table 6 shows the details for backdoor detection.

Table 4: Results for CIFAR-10 in-distribution case (higher number implies higher accuracy). **Boldface** shows the best performing algorithm, whereas underline shows the second best algorithm.

Out-of-Distribution Datasets	Method	TPR95 (%)	AUROC (%)	AUPR (%)
Texture	Ours	58.41	90.97	85.64
	MSP	40.75	88.31	97.08
	Mahalanobis	62.38	94.46	98.75
	Energy Score	47.47	85.47	95.58
	GEM	**72.61**	**94.59**	**98.79**
SVHN	Ours	**88.31**	**96.23**	98.49
	MSP	52.41	92.11	98.32
	Mahalanobis	79.34	95.72	**99.04**
	Energy Score	64.20	91.05	97.66
	GEM	79	95.65	99.01
LSUN-Crop	Ours	79.45	94.33	94.60
	MSP	69.07	95.64	99.13
	Mahalanobis	30.06	86.15	97.05
	Energy Score	**91.89**	**98.40**	**99.67**
	GEM	30.20	86.09	97.03
LSUN-Resize	Ours	69.92	92.03	92.54
	MSP	47.45	91.30	98.11
	Mahalanobis	35.64	88.12	97.45
	Energy Score	**71.75**	**94.12**	**98.64**
	GEM	35.45	88.09	97.43
iSUN	Ours	65.60	90.25	90.33
	MSP	43.40	89.72	97.72
	Mahalanobis	26.77	87.87	97.33
	Energy Score	**66.27**	**92.56**	**98.25**
	GEM	36.80	87.85	93.33
Average Performance	Ours	**72.33**	**92.76**	92.32
	MSP	50.63	91.46	**98.07**
	Mahalanobis	46.83	90.46	97.92
	Energy Score	68.31	92.32	97.96
	GEM	50.81	90.45	97.91

Table 5: Results for CIFAR-100 in-distribution case (higher number implies higher accuracy). **Boldface** shows the best performing algorithm, whereas underline shows the second best algorithm.

Out-of-Distribution Datasets	Method	TPR95 (%)	AUROC (%)	AUPR (%)
Texture	Ours	46.13	87.52	80.57
	MSP	16.71	73.58	93.02
	Mahalanobis	**57.62**	90.14	97.62
	Energy Score	20.38	76.46	93.68
	GEM	57.40	**90.17**	**97.63**
SVHN	Ours	**90.69**	**96.41**	**98.58**
	MSP	15.66	71.37	92.89
	Mahalanobis	51.35	89.25	97.52
	Energy Score	14.59	74.10	93.65
	GEM	51.51	89.40	97.57
LSUN-Crop	Ours	27.93	80.09	79.32
	MSP	33.44	83.71	96.32
	Mahalanobis	1.53	58.48	89.73
	Energy Score	**64.01**	**93.41**	**98.59**
	GEM	1.70	58.42	89.70
LSUN-Resize	Ours	39.80	88.15	86.79
	MSP	16.54	75.32	94.03
	Mahalanobis	**67.20**	93.97	**98.70**
	Energy Score	21.38	79.29	94.97
	GEM	67.09	**94.01**	**98.70**
iSUN	Ours	35.87	86.01	83.37
	MSP	17.02	75.87	94.20
	Mahalanobis	64.07	92.69	**98.32**
	Energy Score	19.20	78.98	94.90
	GEM	**64.10**	**92.73**	**98.32**
Average Performance	Ours	48.08	**87.63**	85.72
	MSP	19.87	75.97	94.09
	Mahalanobis	48.35	84.90	96.37
	Energy Score	27.91	80.44	95.15
	GEM	**48.36**	84.94	**96.38**

Table 6: Comparison results for backdoor detection (higher number implies higher accuracy).

Datasets	Trigger	Metrics (%)	Ours	STRIP	Mahalanobis	GEM	MSP
MNIST	All label	TPR95	83.05	2.58	50.83	**100**	100
		AUROC	**96.13**	44.69	90.78	50.43	50
		AUPR	**94.20**	35.47	86.71	70.94	70.83
MNIST	Naive.1	TPR95	**100**	98.85	99.86	100	5.11
		AUROC	**97.50**	97.32	97.49	53.95	51.64
		AUPR	96.17	95.95	**96.38**	74.74	50.41
MNIST	Naive.2	TPR95	96.53	67.46	35.16	**100**	14.69
		AUROC	**97.28**	93.67	78.63	53.51	58.14
		AUPR	**95.75**	89.85	78.65	74.62	64.16
CIFAR-10	TCA.1	TPR95	**100**	35.68	100	100	4.38
		AUROC	**97.50**	83.00	97.49	50	49.23
		AUPR	95.47	73.22	**97.84**	76.32	52.64
CIFAR-10	TCA.2	TPR95	**100**	27.86	100	100	0.02
		AUROC	**97.50**	68.79	97.49	50	29.90
		AUPR	**97.63**	72.41	95.86	67.86	18.05
CIFAR-10	Wanet	TPR95	37.87	0.07	20.35	22.90	**100**
		AUROC	**92.74**	34.97	50.61	57.81	50
		AUPR	**89.95**	37.42	57.30	68.48	74.87
GTSRB	Moving	TPR95	**99.99**	54	Fail: dependent data dimensions		
		AUROC	**85.39**	7.29			
		AUPR	**96.96**	89.07			
GTSRB	Filter	TPR95	**85.39**	7.29	Fail: dependent data dimensions		
		AUROC	**96.54**	38.92			
		AUPR	**95.42**	38.81			
GTSRB	Wanet	TPR95	**100**	1.24	0.51	100	100
		AUROC	**97.50**	36.31	54.46	50	50
		AUPR	**97.62**	39.53	48.92	75.23	75.23
YouTube Face	Sunglasses	TPR95	73.37	83.03	71.64	**98.58**	13.06
		AUROC	**95.21**	94.80	94.38	84.29	66.55
		AUPR	93.00	**95.54**	94.63	88.83	53.27
YouTube Face	Lipstick	TPR95	**96.64**	90.14	90.88	94.18	3.73
		AUROC	**97.21**	93.15	93.26	80.80	50.14
		AUPR	**96.30**	94.98	95.09	86.53	53.27
sub-ImageNet	Invisible	TPR95	**100**	7.01	0.5	100	51.40
		AUROC	**97.49**	66.26	4.78	50	93.61
		AUPR	**96.53**	62.83	12.27	75.26	92.46
Average Performance		TPR95	89.40	39.60	56.97	**91.57**	39.24
		AUROC	**96.68**	70.30	75.94	58.08	54.92
		AUPR	**95.42**	68.76	76.37	75.88	60.52